

Influence of modification of dental porcelains with hybrid nanomaterial on surface characteristics, antimicrobial, chemical, and mechanical properties

Carla Larissa Vidal

Universidade de Sao Paulo Faculdade de Odontologia de Ribeirao Preto

Izabela Ferreira

Universidade de Sao Paulo Faculdade de Odontologia de Ribeirao Preto

Paulo Sergio Ferreira

Universidade de Sao Paulo Faculdade de Odontologia de Ribeirao Preto

Mariana Lima da Costa Valente

Universidade de Sao Paulo Faculdade de Odontologia de Ribeirao Preto

Ana Beatriz Vilela Teixeira

Universidade de Sao Paulo Faculdade de Odontologia de Ribeirao Preto

Andrea Candido dos Reis (✉ andreare73@yahoo.com.br)

Universidade de São Paulo Faculdade de Odontologia de Ribeirão Preto <https://orcid.org/0000-0002-2307-1720>

Research Article

Keywords: dental porcelain, antimicrobial, nanoparticles, ions, mechanical stress

Posted Date: April 16th, 2020

DOI: <https://doi.org/10.21203/rs.3.rs-22916/v1>

License: © ⓘ This work is licensed under a Creative Commons Attribution 4.0 International License. [Read Full License](#)

Abstract

Evaluated the effect of incorporation of the nanostructured silver vanadate decorated with silver nanoparticles (β -AgVO₃) into dental porcelains on surface characteristics, antimicrobial, chemical, and mechanical properties. The percentages of 2.5% and 5% of β -AgVO₃ were incorporated into commercial dental porcelains IPS Inline and Ex-3 Noritake. Surface characteristics were evaluated by SEM/EDS. Antimicrobial activity were investigated against *Streptococcus mutans*, *Streptococcus sobrinus*, *Aggregatibacter actinomycetemcomitans*, and *Pseudomonas aeruginosa*, by colony counts (CFU/mL), metabolic activity, and multiphoton microscopy. The chemical and mechanical behavior was evaluated by silver (Ag⁺) and vanadium (V⁴⁺/V⁵⁺) ions release, microhardness, roughness, and fracture toughness. Statistical tests Kruskal-Wallis and Dunn's post-hoc were applied for antimicrobial analysis and ions release, and ANOVA and Bonferroni's post-hoc, for mechanical analysis. The nanomaterial interferes in the material's morphology but does not alter the porcelain's components. IPS Inline 5% reduced *S. mutans* and *S. sobrinus* ($p < 0.05$), and Ex-3 Noritake 5% reduced *S. sobrinus* ($p < 0.05$). The IPS Inline 2.5% reduced *A. actinomycetemcomitans* ($p < 0.05$). IPS Inline 5% released more Ag⁺ ($p < 0.05$), and Ex-3 Noritake 2.5% released more V⁴⁺/V⁵⁺ ($p < 0.05$). The β -AgVO₃ increased the fracture toughness of IPS Inline, the roughness for all groups, and decreased the microhardness of 2.5% group ($p < 0.05$). β -AgVO₃ incorporation influenced on morphology but not altered the porcelain's components, promoted antimicrobial activity against *S. mutans*, *S. sobrinus*, and *A. actinomycetemcomitans*, due to the Ag⁺ and V⁴⁺/V⁵⁺ released and influenced the porcelain's mechanical properties.

1. Introduction

Biological complications cause failure in prosthetic rehabilitation with ceramic materials, such as secondary caries initiated by microorganisms like *Streptococcus mutans*, in 40% of cases [1–3], and periodontal disease in 23.7% of rehabilitation with fixed dental prosthesis [4]. Development of dental materials with antimicrobial properties reduce the biofilm formation on the surface of these materials and increase the longevity of restorations, reducing the need for reintervention [5].

Some attempts to add antimicrobials in dental porcelains have been made with the incorporation of silver nanoparticles in feldspathic porcelain [6] and into zirconia for dental implant applications [7], antimicrobial glass coatings applications [8], and aluminum particles in ceramic compounds [9].

Vanadates, compounds that contain vanadium in its highest oxidation state, allow intercalation with other elements, resulting in the synthesis of nanostructures with different compositions and properties. Recently, the nanostructured silver vanadate decorated with silver nanoparticles (β -AgVO₃), a hybrid system based on vanadate nanowires and silver nanoparticles was introduced [10]. This nanomaterial dissociates into silver (Ag⁺) and vanadium (V⁴⁺ and V⁵⁺) ions and act on bacterial structures [10, 11].

In dentistry, the β -AgVO₃ was incorporated in several dental materials such as acrylic resins, denture liners, impression materials, endodontic sealers, and prosthetic components, and demonstrated antimicrobial activity against *Streptococcus mutans*, *Candida albicans*, *Staphylococcus aureus*, *Pseudomonas aeruginosa*, *Enterococcus faecalis* and *Escherichia coli* [12–19].

A recent study that incorporated the β -AgVO₃ into dental porcelains indicated a promising antibacterial effect against *S. mutans* through agar diffusion method [20]. However, studies that prove the antimicrobial effectiveness against several species of microorganisms and the influence of this nanomaterial on the other characteristics and properties of these dental porcelains have not yet been realized.

Given the successful use of β -AgVO₃ into these dental materials, the purpose of the present study was to incorporate this nanomaterial into dental porcelains and investigate the surface characteristics, antimicrobial, chemical, and mechanical properties. The hypothesis tested was that the β -AgVO₃ incorporation does not influence on surface characteristics, antimicrobial, chemical, and mechanical properties of dental porcelains tested.

2. Experimental Section

2.1. Specimen preparation

The synthesis of the nanostructured silver vanadate decorated with silver nanoparticles ($\beta\text{-AgVO}_3$) was performed according to Holtz et al. [11] and Castro et al. [12]. Briefly, 0.9736 g of ammonium metavanadate (NH_4VO_3 ; 99%; Merck KGaA, Darmstadt, Germany) and 1.3569 g of silver nitrate (AgNO_3 ; 99,8%; Merck KGaA) were solubilized separately in 200 mL of distilled water. A solution was added to the other, obtaining the silver vanadate solution, which was vacuum filtered, washed with distilled water and absolute ethanol, and dried in vacuum for 10 hours to give $\beta\text{-AgVO}_3$ powder.

Two commercial dental porcelains were used: IPS Inline (Ivoclar Vivadent, Schaan, Liechtenstein) and Ex-3 Noritake (Noritake Kizai CO., Nagoya, Japan) in A3 color for dentin. The $\beta\text{-AgVO}_3$ was added in concentrations of 2.5 and 5 wt%. A control group was obtained with the commercial dental porcelains, which were manipulated according to the manufacturer's instructions. To the modified groups, the powder of the dental porcelains was considered 100% and the mass (wt%) corresponding to the nanomaterial concentrations (2.5% and 5%) were subtracted of the powder and the $\beta\text{-AgVO}_3$ concentration were added. The powder was deposited in a Teflon matrix (8 × 2 mm), then removed and prepared for oven processing. The specimens were fired over refractory wool (initial temperature of 403 °C, heating rates of 60 °C/minute, and firing temperature of 910 °C for IPS Inline and initial temperature of 600 °C, heating rates of 45 °C/minute, and firing temperatures of 920 °C for Ex-3 Noritake). After firing, the furnace door was opened only 10% until the temperature inside the oven reached 300°C, whereupon it was opened completely. The specimens were then submitted to a second firing (900 °C), following a fast cooling protocol (45 and 60 °C/second respectively). Thus, six groups were obtained: IPS Inline control (commercial porcelain, without $\beta\text{-AgVO}_3$), IPS Inline 2.5% of $\beta\text{-AgVO}_3$, IPS Inline 5% of $\beta\text{-AgVO}_3$, Ex-3 Noritake control (commercial porcelain, without $\beta\text{-AgVO}_3$), Ex-3 Noritake 2.5% of $\beta\text{-AgVO}_3$, Ex-3 Noritake 5% of $\beta\text{-AgVO}_3$. After, they were polished with water sandpaper for surface planning and sterilized with ethylene oxide for microbiological assays.

2.2. Surface characteristics and chemical composition

The surface characterization of the specimens (n = 2) and elemental microanalysis was carried out using energy-dispersive X-ray spectroscopy (EDS - IXRF Systems mod. 500 Digital Processing, Houston, USA) coupled to a Scanning Electron Microscopy (SEM - ZEISS model EVO 50, Cambridge, United Kingdom) with a 20 kV electron beam, using SE and BSD detectors for topographic and compositional evaluations, respectively. To increase the conductivity, specimens were gold-sputtered. Microanalysis was performed at a working distance of 8.5 mm, Iprobe at 20 nA, and dead time at approximately 30% in 300x magnification, and the photomicrographs were obtained at 300, 1 k, 5 k, 10 k, 30 k, 50 k, and 100 k x magnifications.

2.3. Antimicrobial activity

The $\beta\text{-AgVO}_3$ minimum inhibitory concentration (MIC) against *Streptococcus mutans* (ATCC 25175), *Streptococcus sobrinus* (ATCC 33402), *Aggregatibacter actinomycetemcomitans* (ATCC 33384), and *Pseudomonas aeruginosa* (ATCC 27853) was performed by the method of successive dilutions described by the Clinical and Laboratory Standards Institute [21], in 96-well plates. The plates were prepared with the culture medium supplemented with decreasing concentrations of the nanomaterial. Each well was inoculated with the microorganism under testing, and after 24 hours of incubation, the bacteriostatic effect of the material was assessed by the turbidity of the culture visible to the naked eye. Ten concentrations of the nanomaterial and two control groups were obtained: one positive, with microorganism and culture medium, and another negative, with $\beta\text{-AgVO}_3$ and sterile culture medium [12].

To biofilm formation, microorganisms were obtained from a recent culture and standardized in spectrophotometer (PCB 687, BYK Gardner GMBH, Geretsried, Germany) at a wavelength of 625 nm and a concentration of 10^8 CFU/mL bacteria. Specific culture mediums for each microorganism was used (modified SB-20 for *S. mutans*, *S. sobrinus*, and *P. aeruginosa* and Tryptic Soy Broth for *A. actinomycetemcomitans*). Specimens (n = 10) were inserted into 24-wells plates and 1000 μL of the culture medium inoculated was added to each well, and a negative control group was used with one specimen for each group and sterile culture medium. The plates were incubated at 37 °C for 1 h 30 min under stirring at 750 rpm (Shaker, Cienlab, Campinas, SP, Brazil) for adhesion. Then the specimens were rinsed with saline solution and 1000 μL of sterile culture medium was added. The plates were incubated for 48 h under the same conditions for growth and maturation biofilm [13].

The cell viability of the microorganisms was quantified by colony forming units per milliliter (CFU/mL) and metabolic activity. For CFU/mL, after biofilm formation, each specimen was washed, added to a microtube containing 1000 μL of PBS and sonicated in an ultrasonic bath (Altsonic, Clean 9CA, Ribeirão Preto, SP, Brazil) (200 watts/40 Hz) for 20 min. Afterward, 25 μL was collected and serial dilutions (10^{-1} to 10^{-4}) were seeded in specific culture medium and incubating at 37 °C for 24 hours ($n = 10$). The CFU/mL was counted. The metabolic activity was evaluated by XTT Cell Viability Assay Kit (Uniscience, São Paulo, Brazil). After biofilm formation, each specimen was washed and 50 μL of XTT solution was placed in each well ($n = 10$). The plates were incubated in the dark at 37 °C for 2 hours. Then, 100 μL aliquots of the homogenized suspension from each well were transferred to 96-well plates, in triplicate, and quantified the crystal formazan formation by spectrophotometry at 492 nm using a microplate reader (Synergy II, BioTek Instruments, Winooski, VT, USA) [13].

Qualitative analysis of biofilms was performed using multiphoton microscopy. After biofilm formation, each specimen was washed ($n = 2$) and stained with 300 μL of Live / Dead® BacLight™ L 7007 dye (Molecular Probes, Inc., Eugene, OR, USA), for 15 minutes protected from light. The specimens were evaluated using a Zeiss LSM-7MP multiphoton microscope (Carl Zeiss, Oberkochen, Germany). Two-photon images were acquired selecting an area of 4 \times 4 mm at the center of biofilm and analyzed using ZEN LSM (Carl Zeiss) and Image J (National Institutes of Health, Bethesda, MD, USA) software.

2.4. Silver and Vanadium Ions Release

The release of silver (Ag^+) and vanadium ($\text{V}^{4+}/\text{V}^{5+}$) ions was assessed by atomic absorption spectroscopy (Varian AA240FS, Varian Inc., Palo Alto, California, USA). The specimens ($n = 3$) were immersed in tubes with 10 mL of deionized water, kept at 37°C under agitation in an orbital shaker (Tecnal TE 420, Tecnal Scientific Equipment, Piracicaba, São Paulo, Brazil), with 6 hours of agitation per day, for 7, 30 and 120 days. The Ag^+ and $\text{V}^{4+}/\text{V}^{5+}$ ions were quantified by collecting 1 mL of each tube, by calibration curves built in the equipment.

2.5. Mechanical tests

For the evaluation of mechanical behavior, the surface roughness ($n = 10$) was carried out using the rugosimeter SurfTest SJ-201P (Mitutoyo Corporation, Japan) according to technical standard NBR ISO 4287:2002. The analyzer tip touched the piece and covered a distance of 4 mm, making three measurements on each specimen in the direction of its larger diameter. The surface microhardness ($n = 10$) was measured through a microdurometer (Shimadzu HMV-2, Japan) with a Vickers type indenter with a load of 0.2 Kgf for 20 s. Three readings were performed in different regions for each specimen. The Vickers indentation method was used for analyzed fracture toughness ($n = 10$). Each print featured two pairs of radial cracks. Thirty pairs of perfect cracks were used (without polishing imperfections and trajectory deviations). Fracture toughness values were calculated using the equation proposed by Antis: $K_{IC} = 0.016 (E/H)^{1/2} P/C^{3/2}$. Where: K_{IC} = material fracture toughness ($\text{MPa}\cdot\text{m}^{1/2}$); E = modulus of elasticity of material (GPa); H = material hardness (GPa); l = crack length (m); P = applied load (N); $C = 1 + a$ (m); a = semi-diagonal of the Vickers impression (m).

2.6. Statistical Analysis

After verifying the distribution of data using the Shapiro-Wilk test ($\alpha = 0.05$), statistical tests Kruskal-Wallis and Dunn's post-hoc were applied for antimicrobial analysis and ions release, and ANOVA and Bonferroni's post-hoc, for mechanical analysis. The SEM/EDS and multiphoton microscopy data were analyzed qualitatively.

3. Results

3.1. Surface characteristics and chemical composition

The control group of IPS Inline feldspathic porcelain showed few irregularities on the surface, with some aluminum and silicon peaks (Fig. 1a). When the $\beta\text{-AgVO}_3$ was incorporated, greater surface roughness was observed. For IPS Inline 2.5% deeper pores and peaks were observed (Fig. 1b), and for IPS Inline 5%, steeper peaks were observed (Fig. 1c). The Ex-3 Noritake control group showed more peaks and pores than IPS Inline control group (Fig. 1d). With the $\beta\text{-AgVO}_3$ incorporation, a considerable increase in surface irregularities was observed. The Ex-3 Noritake 2.5% presented high surface roughness and surface morphology distinct

from the control group (Fig. 1e), and the 5% group showed more peaks and deeper pores (Fig. 1f). The elemental analysis by EDS showed higher oxygen and slightly lower potassium and zinc levels for IPS Inline when compared to Ex-3 Noritake (Table 1). Both groups incorporated with 5% β -AgVO₃ showed a higher percentage of silver and vanadium ions than groups incorporated with 2.5% β -AgVO₃ (Table 1). In general, the atomic percentage of chemical elements present in dental porcelains did not change with the incorporation of the nanomaterial.

Table 1
Chemical elements detected in commercial dental porcelains incorporated with β -AgVO₃ using energy-dispersive X-ray spectroscopy (EDS) (wt.%).

| Chemical element | IPS Inline | | | Ex-3 Noritake | | |
|------------------|------------|-------|-------|---------------|-------|-------|
| | control | 2.5% | 5% | control | 2.5% | 5% |
| C | 0.00 | 0.00 | 0.00 | 0.00 | 0.00 | 0.00 |
| O | 45.46 | 44.47 | 44.02 | 44.88 | 42.79 | 43.88 |
| Al | 8.51 | 8.71 | 8.08 | 8.14 | 7.95 | 7.87 |
| Si | 29.20 | 29.48 | 28.33 | 29.16 | 31.87 | 29.07 |
| P | 0.00 | 0.00 | 0.00 | 0.00 | 0.02 | 0.00 |
| S | 0.00 | 0.00 | 0.00 | 0.00 | 0.02 | 0.00 |
| Cl | 0.02 | 0.00 | 0.00 | 0.03 | 0.00 | 0.08 |
| K | 8.93 | 8.73 | 8.65 | 7.40 | 6.53 | 6.98 |
| Ca | 0.86 | 0.83 | 0.81 | 0.56 | 0.69 | 0.57 |
| Fe | 0.05 | 0.08 | 0.05 | 0.04 | 0.02 | 0.04 |
| Zn | 6.73 | 7.02 | 6.90 | 9.73 | 9.01 | 9.07 |
| Ag | 0.25 | 0.40 | 2.40 | 0.05 | 0.53 | 1.78 |
| V | 0.00 | 0.27 | 0.75 | 0.00 | 0.58 | 0.64 |

3.2. Antimicrobial activity

The minimum inhibitory concentration of β -AgVO₃ necessary to inhibit the growth of microorganisms *S. mutans*, *S. sobrinus*, and *A. actinomycetemcomitans* was 250 μ g/mL, and for *P. aeruginosa*, was 31.25 μ g/mL (Table 2). When incorporated into IPS Inline caused a reduction in cell viability of *S. mutans* ($p < 0.05$). 5% β -AgVO₃ also reduced the metabolic activity of *S. sobrinus* when incorporated into Ex-3 Noritake, and the CFU/mL when incorporated into IPS Inline ($p < 0.05$). The incorporation of 2.5% β -AgVO₃ into IPS Inline showed antibacterial effect on the metabolic activity of *A. actinomycetemcomitans* ($p < 0.05$). The other concentrations of β -AgVO₃ incorporated into IPS Inline and Ex-3 Noritake showed no antimicrobial effect against *A. actinomycetemcomitans* and *P. aeruginosa* ($p > 0,05$) (Table 2).

Table 2

Minimum inhibitory concentration (MIC) of pure β -AgVO₃ and antimicrobial activity of dental porcelains incorporated with β -AgVO₃ on metabolic activity and colony forming units per milliliter (CFU/mL) of microorganisms.*

| Microorganisms | MIC of β -AgVO ₃ (µg/mL) | Group | Metabolic activity (nm) | | CFU/mL | |
|----------------|---|---------|------------------------------------|------------------------------------|-----------------------------------|-----------------------------------|
| | | | IPS Inline | Ex-3 Noritake | IPS Inline | Ex-3 Noritake |
| <i>S. m</i> | 250 | Control | 0.91 [0.77;1.16] ^{Aa} | 0.24 [0.19;0.49] ^{Ba} | 7.60 [7.25;7.88] ^{Aa} | 6.78 [6.58;7.23] ^{Ba} |
| | | 2.5% | 0.67 [0.47;0.95] ^a | 0.55 [0.45;0.79] ^b | 5.71 [3.50;7.16] ^{ab} | 7.40 [6.18;7.95] ^a |
| | | 5% | 0.12 [0.06;0.22] ^b | 0.22 [0.12;0.30] ^a | 5.13 [4.03;5.98] ^{Ab} | 7.04 [6.31;7.24] ^{Ba} |
| <i>S. s</i> | 250 | Control | 1.04 [0.82;1.21] ^a | 0.97 [0.86;1.08] ^a | 8.21 [7.74;8.44] ^a | 8.14 [7.63;8.69] |
| | | 2.5% | 1.17 [0.77;1.40] ^{Aa} | 0.97 [0.70; 1.16] ^{Ba} | 8.19 [5.22;9.02] ^{ab} | 7.82 [7.61;8.28] |
| | | 5% | 1.06 [0.76;1.29] ^{Aa} | 0.82 [0.57;1.01] ^{Bb} | 7.03 [4.45;7.90] ^{Ab} | 7.89 [6.81;8.47] ^B |
| <i>A. a</i> | 250 | Control | 1.10 [1.06;1.12] ^{Aa} | 1.17 [1.14;1.24] ^{Ba} | 7.30 [7.03/7.35] ^a | 7.17 [7.10;7.27] ^{ab} |
| | | 2.5% | 1.00 [0.98;1.05] ^{Ab} | 1.20 [1.16;1.30] ^{Ba} | 7.37 [7.25;7.48] ^{ab} | 7.44 [7.17;7.55] ^a |
| | | 5% | 1.12 [1.03;1.23] ^{ab} | 1.18 [1.16;1.20] ^a | 7.39 [7.27;7.47] ^{Ab} | 7.14 [7.03;7.23] ^{Bb} |
| <i>P. a</i> | 31.25 | Control | 0.23 [0.13;0.41] ^a | 0.09 [0.06;0.18] ^a | 6.82 [6.29;7.61] | 6.37 [6.11;7.59] |
| | | 2.5% | 0.50 [0.35;0.94] ^b | 0.92 [0.53;1.14] ^b | 7.44 [6.63;8.14] | 7.19 [6.70;8.07] |
| | | 5% | 0.31 [0.28;0.41] ^{Aab} | 0.58 [0.39;0.75] ^{Bc} | 6.46 [6.11;8.31] | 6.17 [5.27;7.59] |

**S. m* = *Streptococcus mutans*; *S. s* = *Streptococcus sobrinus*; *A. a* = *Aggregatibacter actinomycetemcomitans*; *P. a* = *Pseudomonas aeruginosa*. Kruskal-Wallis, Dunn's post-hoc and Mann-Wittney tests ($\alpha = 0.05$). Median [confidence interval]. ^{a,b} Equal lowercase letters in the same column indicate statistical similarity ($p > 0.05$). ^{A,B} Equal uppercase letters in the same row for each method indicate statistical similarity ($p > 0.05$).

The photon images of biofilms formed on the surface of dental porcelains incorporated with different concentrations of β -AgVO₃ are in agreement with the results observed in the microbiology analysis. In Fig. 2, it was observed that the IPS Inline 2.5% β -AgVO₃ group (Fig. 2b) presented *S. mutans* biofilm thicker with clusters of non-viable cells surrounded by viable cells, showing a different pattern from the control group (Fig. 2a). Clusters also were observed in *S. sobrinus* biofilm formed on the surface of the 5% IPS Inline group (Fig. 2d), and with a higher proportion of non-viable cells compared to the control group (Fig. 2c). On the surface of the IPS Inline 2.5% group (Fig. 2f), it was observed a lower proportion of viable cells than the control group (Fig. 2e) for *A. actinomycetemcomitans* biofilm. For Ex-3 Noritake groups, it was observed an *S. sobrinus* thicker biofilm with the incorporation of 5% β -AgVO₃ (Fig. 3b), with a higher proportion of non-viable cells compared to the control group (Fig. 3a). Despite the quantitative results for *P. aeruginosa*, the photon images demonstrated a higher proportion of non-viable cells in Ex-3 Noritake incorporated with 5% (Fig. 3d) compared to the control group (Fig. 3c).

3.3. Silver and Vanadium Ions Release

The group incorporated with 5% $\beta\text{-AgVO}_3$ of IPS Inline presented the highest Ag^+ release ($p < 0.05$). Ex-3 Noritake porcelain incorporated with 2.5% nanomaterial, presented the highest release of $\text{V}^{4+}/\text{V}^{5+}$ ($p < 0.05$), in 7 days. No statistical difference was found for the release of $\text{V}^{4+}/\text{V}^{5+}$ between the groups modified by the nanomaterial at 30 and 120 days ($p > 0.05$). In general, the groups released more $\text{V}^{4+}/\text{V}^{5+}$ than Ag^+ , and within the same group, there were no variations in the release of $\text{V}^{4+}/\text{V}^{5+}$ and Ag^+ over time ($p > 0.05$) (Table 3).

Table 3
– Different times of silver and vanadium ions release of dental porcelains incorporated with $\beta\text{-AgVO}_3$.*

| Porcelain | Group | Ag^+ | | | $\text{V}^{4+}/\text{V}^{5+}$ | | |
|--|---------|-------------------------------------|-------------------------------------|-------------------------------------|--------------------------------------|-------------------------------------|-------------------------------------|
| | | 7 days | 30 days | 120 days | 7 days | 30 days | 120 days |
| Ex-3 Noritake | Control | 0 ^{Aa} | 0 ^{Aa} | 0 ^{Aa} | 0 ^{Aa} | 0 ^{Aa} | 0 ^{Aa} |
| | 2.5% | 0.22 [0.07;0.43] ^{Abc} | 0.23 [0.10;0.39] ^{Abc} | 0.25 [-0.14;0.75] ^{Abc} | 14.65 [-1.44;25.68] ^{Ab} | 10.92 [6.67;14.49] ^{Ab} | 2.64 [0.63;4.25] ^{Ab} |
| | 5% | 0.26 [-0.05;0.54] ^{Abc} | 0.12 [-0.04;0.33] ^{Abc} | 0.16 [-0.13;0.53] ^{Abc} | 2.52 [1.18;4.47] ^{Ac} | 1.98 [-0.27;4.82] ^{Ab} | 3.99 [0.58;7.67] ^{Ab} |
| IPS Inline | Control | 0 ^{Aab} | 0 ^{Aab} | 0 ^{Aab} | 0 ^{Aa} | 0 ^{Aa} | 0 ^{Aa} |
| | 2.5% | 0.32 [-0.56;0.60] ^{Abc} | 0.08 [-0.40;0.83] ^{Abc} | 0.08 [-0.21;0.46] ^{Abc} | 4.79 [0.61;7.53] ^{Abc} | 4.24 [-4.70;16.20] ^{Ab} | 5.33 [-2.87;13.11] ^{Ab} |
| | 5% | 0.45 [-0.06;1.20] ^{Ac} | 0.41 [0.02;0.81] ^{Ac} | 0.53 [-0.25;1.24] ^{Ac} | 5.95 [-6.06;22.27] ^{Abc} | 12.71 [2.11;20.13] ^{Ab} | 1.31 [-2.41;6.93] ^{Ab} |
| *Kruskal-Wallis and Dunn's post-hoc tests ($\alpha = 0.05$). Median [confidence interval]. ^{a,b} Equal lowercase letters in the same column indicate statistical similarity ($p > 0.05$). ^{A,B} Equal uppercase letters in the same row indicate statistical similarity for each ion ($p > 0.05$). | | | | | | | |

3.4. Mechanical tests

The incorporation of $\beta\text{-AgVO}_3$ into dental porcelains influenced the mechanical behavior of these materials. The surface roughness increased with the nanomaterial incorporation, the 5% $\beta\text{-AgVO}_3$ group was statistically different from IPS Inline ($p = 0.045$) and Ex-3 Noritake ($p = 0.036$) control groups. The incorporation of 2.5% $\beta\text{-AgVO}_3$ decreased the microhardness compared to the control ($p < 0.001$) and 5% ($p = 0.014$) groups, that did not differ from each other. In IPS Inline, the $\beta\text{-AgVO}_3$ incorporation increased the fracture toughness, mainly for the 5% group ($p < 0.001$). For Ex-3 Noritake, there was no difference between groups ($p = 1.000$) (Table 4).

Table 4
Mechanical behavior of dental porcelains incorporated with β -AgVO₃.*

| Porcelain | Group | Roughness (μm) | Microhardness HV (Kgf/cm ²) | Fracture toughness (MPa.m ^{1/2}) |
|---------------|---------|-----------------------------|---|--|
| Ex-3 Noritake | Control | 1.74 (1.44) ^a | 609.50 (62.07) ^a | 0.18 (0.41) ^a |
| | 2.5% | 3.04 (1.30) ^{ab} | 497.20 (65.55) ^b | 0.20 (0.41) ^a |
| | 5% | 3.56 (2.01) ^b | 571.50 (86.04) ^a | 0.19 (0.65) ^a |
| IPS Inline | Control | 1.76 (0.72) ^a | 542.46 (23.96) ^a | 0.19 (0.03) ^a |
| | 2.5% | 3.37 (1.35) ^{ab} | 503.10 (48.60) ^b | 1.86 (0.25) ^b |
| | 5% | 3.51 (2.09) ^b | 535.83 (36.93) ^a | 2.40 (0.49) ^c |

*ANOVA and Bonferroni's post-hoc tests ($\alpha = 0.05$). Mean and standard deviation. ^{ab} Equal lowercase letters in the same column indicate statistical similarity for each dental porcelain ($p > 0.05$).

4. Discussion

This study used two commercial feldspathic dental porcelains, IPS Inline and Ex-3 Noritake, to evaluate the viability of the mixture between ceramic materials and the β -AgVO₃ nanomaterial in an unprecedented way. One of the biggest challenges in incorporating antimicrobial compounds into ceramic materials is that the material is exposed to high temperatures during processing, which may impair the action of the added compound [22]. Positive results were obtained in this study, once the chemical composition confirmed the viability of the proposed mixture, with the unaltered atomic proportion of the porcelain elements, added to the beneficial antimicrobial effect of the β -AgVO₃ addition, without major damage to the mechanical properties. Thus, the null hypothesis tested in this study was rejected.

The β -AgVO₃ antimicrobial effect observed is due to the action of silver (Ag⁺) and vanadium (V⁴⁺ and V⁵⁺) ions released by the nanomaterial in contact with bacterial surfaces [10, 11]. Ag⁺ adheres to the cytoplasmic membrane or cell wall through electrostatic interaction with sulfur proteins, which can permeate the membrane and cause its rupture [23]. Vanadium ions in the 5+ state of oxidation and Ag⁺ interact with the thiol groups present in the enzyme's bacterial metabolism, forming stable complexes. Ag⁺ still comes into contact with bacterial DNA preventing their replication, and oxidation-reduction between V⁴⁺ and V⁵⁺ leads to oxidative stress in the bacterial cell [11].

The pure β -AgVO₃ demonstrated antimicrobial activity confirming its potential to be used as an antimicrobial agent, as observed in other studies [12, 17]. When incorporated into dental porcelains, it presented more effect against *S. mutans* and *S. sobrinus*, demonstrating a spectrum of action against Gram-positive and Gram-negative bacteria, which can prevent the incidence of dental caries. Oda et al. [24] related that in the presence of *S. mutans* and *S. sobrinus* the incidence of the dental caries is significantly higher than when in the presence of *S. mutans* only. The IPS Inline with 5% of β -AgVO₃ presented higher action against *S. mutans* than *S. sobrinus*, which can be due to the greater resistance of the *S. sobrinus* whose virulence and acid-forming capacity is higher and faster than *S. mutans* [25, 26]. A positive effect against *S. sobrinus* was observed to Ex-3 Noritake incorporated with 5% of β -AgVO₃.

IPS Inline with 2.5% of β -AgVO₃ showed antimicrobial activity against *A. actinomycetemcomitans*. This microorganism is commonly found in aggressive periodontal disease [27, 28], and may cause extraoral infections such as infectious endocarditis, bacterial arthritis, pregnancy-associated septicemia, brain abscesses, and osteomyelitis, but its primary source is the oral cavity [28]. *Acinetobacter spp.* associate with *P. aeruginosa* participate in the etiopathogenesis of periodontal diseases and, *P. aeruginosa*, *A. actinomycetemcomitans*, *A. baumannii* and species of the red complex (*Porphyromonas gingivalis*, *Tannerella forsythia*, and *Treponema denticola*), increase the likelihood of developing aggressive periodontitis [29]. Against *P. aeruginosa*, the modified porcelains showed no antimicrobial activity. The resistance of *A. actinomycetemcomitans* and *P. aeruginosa*, both of

which are Gram-negative, to the action of $\beta\text{-AgVO}_3$ can be due to structural differences, as they have an additional external membrane that Gram-positive bacteria do not possess, resulting in different susceptibility and permeability to antimicrobial agents [30].

The pure $\beta\text{-AgVO}_3$ demonstrated higher antimicrobial activity than when was incorporated into dental porcelains, mainly to *P. aeruginosa*. This can be due to the total non-release of the nanomaterial when incorporated, once all groups released more vanadium ions than silver ions. However, in the synthesis of the nanomaterial, 2 mmol of silver nitrate is added while 1 mmol of ammonium metavanadate is added [11], thus expecting a greater release of silver. This greater release of vanadium than silver was also observed in other dental materials incorporated with $\beta\text{-AgVO}_3$ [31, 32].

The results also demonstrated that the IPS Inline presented better antimicrobial effect than Ex-3 Noritake. This difference can be due to the greater release of silver and vanadium ions by IPS Inline, and due to differences in this porcelain's sintering cycle led to a change in the nanomaterial's properties. During processing, Ex-3 Noritake reaches temperatures of 600 °C, as indicated by the manufacturer, whereas IPS Inline is limited to 403 °C. The high temperatures produced during porcelain sintering negatively impact the incorporation of antimicrobial agents [22]. In addition, the porcelain's composition (Ex-3 Noritake presented less K and more Zn wt.% elements) and particle type may not have interacted or integrated with the nanomaterial and may have therefore inhibited effective antimicrobial release.

The $\beta\text{-AgVO}_3$ incorporation changed the surface characteristics and higher roughness was observed. This higher roughness may have provided biofilm retention in the groups that did not show a reduction in the bacterial contingent. The roughness has a considerable influence on biofilm formation because it favors greater quantity and early maturation of bacteria that are lodged in pores [33]. Despite the higher roughness, the nanomaterial released demonstrated antimicrobial effect in some groups.

Roughness is also related to mechanical microretention between the cementing agent and the porcelain and is positively correlated with bond strength [34]. The proposed new material can be used on the inner face of porcelain restorations; thus, it may enhance their mechanical retention [35].

The photomicrographs of surface characteristics suggest that the incorporation interfered more in the material conformation when compared to the control groups and indicate that this interference was different from one porcelain to another, which corroborates the mechanical and antimicrobial results. Morphology may also have interfered with antimicrobial potential due to nanomaterial dispersion. When used in conjunction with SEM, dispersive EDS is a chemical microanalysis technique that facilitates the investigation of various samples' compositional details [36]. Based on this analysis, the porcelains presented few differences in oxygen, potassium and zinc levels. The presence of silver and vanadium in the groups incorporated with $\beta\text{-AgVO}_3$ indicates the presence of the nanomaterial in the new material's structure, and this addition without changing the components inherent to the porcelain itself.

Several parameters, such as microhardness and fracture toughness, influence the porcelain's mechanical properties and clinical use. A lower fracture toughness value can lead to poorer clinical performance [37]. When this property was evaluated, the incorporation of the nanomaterial in IPS Inline promoted an increase of fracture toughness, which can lead to a considerable increase in the material's ability to absorb elastic energy, indicating a greater chance of surviving more severe impacts [38]. The fracture toughness values for the modified groups of IPS Inline are in accordance with results showed in literature for feldspathic porcelains [38]. In microhardness evaluation, the group incorporated with 2.5% presented the lowest value. However, this property did not change in the group incorporated with 5% $\beta\text{-AgVO}_3$, demonstrating that the incorporation of higher concentrations of vanadate does not harm the mechanical properties and still favors the antimicrobial effectiveness.

Significant results were obtained by incorporating $\beta\text{-AgVO}_3$ into dental porcelains, including imbuing materials with antimicrobial properties against microorganisms frequently associated with dental problems. Thus, the antimicrobial action identified in this study has high significance, as the nanomaterial was able to maintain its effectiveness after porcelain processing. Improving the fracture toughness property of IPS Inline and maintaining this property for Ex-3 Noritake through the incorporation of the nanomaterial suggests the possible viability of this material for clinical application. The porcelains used are commercial

formulations, so this study is an initial analysis of the viability of mixing porcelain materials and β -AgVO₃. Therefore, the development of specific formulations to receive this additive should be evaluated in the future.

This study has its limitations because it was performed strictly *in vitro*. The interaction between microorganisms *in vivo* may lead to different results, and further analysis is important to consider the clinical use of these porcelains.

Although the results regarding the mechanical properties were altered, the literature is not clear about the maximum acceptable alteration levels. Because the suggested use of this material is limited to the internal regions of prostheses, achieving antimicrobial results after firing processing, as well as processing the modified material itself and giving it shape, contour and strength, shows the great advance and potential use that this methodological proposal offers.

5. Conclusions

The β -AgVO₃ incorporation into dental porcelains did not alter the inherent components of the porcelain itself and promoted antimicrobial activity in IPS Inline against *S. mutans*, *S. sobrinus*, and *A. actinomycetemcomitans*. The dental porcelains incorporated with the nanomaterial released more vanadium than silver ions, and increased the surface roughness, not affect microhardness of 5% group and the increased fracture toughness of IPS Inline.

Declarations

Acknowledgements

This work was supported by the Foundation for Research Support of the State of São Paulo [grant number 2018/03447-0]; and Coordination for the Improvement of Higher Education Personnel [grant number 001].

The authors declare that they have no conflict of interests

References

1. Abduo J, Sambrook RJ. Longevity of ceramic onlays: A systematic review. *J Esthet Restor Dent*. 2018;30:193–215.
2. Araujo NS, Moda MD, Silva EA, et al. Survival of all-ceramic restorations after a minimum follow-up of five years: A systematic review. *Quintessence Int*. 2016;47:395–405.
3. Castillo-Oyagüe R, Sancho-Esper R, Lynch CD, et al. All-ceramic inlay-retained fixed dental prostheses for replacing posterior missing teeth: A systematic review. *J Prosthodont Res*. 2018;62:10–23.
4. Zafar N, Ghani F. Common post-fitting complications in tooth-supported fixed-fixed design metal-ceramic fixed dental prostheses. *Pak J Med Sci*. 2014;30:619–25.
5. Amaral GS, Negrini T, Maltz M. M, et al. Restorative materials containing antimicrobial agents: is there evidence for their antimicrobial and anticaries effects? A systematic review. *Aust Dent J*. 2016;61:6–15.
6. Kim JH, Park SW, Lim HP, et al. Biocompatibility evaluation of feldspathic porcelain with nano-sized silver ion particles. *J Nanosci Nanotechnol*. 2018;18:1237–40.
7. Xu K, Liu Y, Liu S, et al. Microorganism adhesion inhibited by silver doped yttria-stabilized zirconia ceramics. *Ceram Int*. 2011;37:2109–15.
8. Llama-Palacios A, Sánchez MC, Díaz LA, et al. In vitro biofilm formation on different ceramic biomaterial surfaces: Coating with two bactericidal glasses. *Dent Mater*. 2019;35:883–92.
9. Saravia SGG, Rastelli SE, Ortega-Avilés M, et al. Physical, mechanical properties and antimicrobial analysis of a novel CaO·Al₂O₃ compound reinforced with Al or Ag particles. *J Mech Behav Biomed Mater*. 2019;97:385–95.
10. Holtz RD, Souza Filho AG, Brocchi M, et al. Development of nanostructured silver vanadates decorated with silver nanoparticles as a novel antibacterial agent. *Nanotechnology*. 2010;21:1–8.
11. Holtz RD, Lima BA, Souza Filho AG, et al. Nanostructured silver vanadate as a promising antibacterial additive to water-based paints. *Nanomedicine*. 2012;8:935–40.

12. Castro DT, Holtz RD, Alves OL, et al. Development of a novel resin with antimicrobial properties for dental application. *J Appl Oral Sci.* 2014;22:442–9.
13. Castro DT, Valente MLC, Agnelli JA, et al. In vitro study of the antibacterial properties and impact strength of dental acrylic resins modified with a nanomaterial. *J Prosthet Dent.* 2016;115:238–46.
14. Castro DT, Valente MLC, Silva CHL, et al. Evaluation of antibiofilm and mechanical properties of new nanocomposites based on acrylic resins and silver vanadate nanoparticles. *Arch Oral Biol.* 2016;67:46–53.
15. Kreve S, Oliveira VC, Bachmann L, et al. Influence of AgVO₃ incorporation on antimicrobial properties, hardness, roughness and adhesion of a soft denture liner. *Sci Rep.* 2019;9:1–9.
16. Castro DT, Kreve S, Oliveira VC, et al. Development of an impression material with antimicrobial properties for dental application. *J Prosthodont* 2019; **2019**: 1–7.
17. Teixeira ABV, Vidal CL, Castro DT, et al. Incorporating antimicrobial nanomaterial and its effect on the antimicrobial activity, flow and radiopacity of endodontic sealers. *Eur Endod J.* 2017;2:1–8.
18. Teixeira ABV, Vidal CL, Albiasseti T, et al. Influence of adding nanoparticles of silver vanadate on antibacterial effect and physicochemical properties of endodontic sealers. *Iran Endod J.* 2019;14:7–13.
19. Oliscovicz NF, Castro DT, Valente MLC, et al. Surface treatment of implant materials with antimicrobial nanoparticles. *Gen Dent* 2018; 66–73.
20. Ferreira I, Vidal CL, Botelho AL, et al. Effect of nanomaterial incorporation on the mechanical and microbiological properties of dental porcelain. *J Prosthet Dent.* 2020;123:529.e1-e5.
21. Clinical and Laboratory Standards Institute (CLSI). *Methods for dilution antimicrobial susceptibility tests for bacteria that grow aerobically*, 6th ed, 2003.
22. Yoshida H, Abe H, Taguri T, et al. Antimicrobial effect of porcelain glaze with silver-clay antimicrobial agent. *J Ceram Soc Jpn.* 2010;118:571–4.
23. Abbaszadegan A, Ghahramani Y, Gholami A, et al. The effect of charge at the surface of silver nanoparticles on antimicrobial activity against Gram-positive and Gram-negative bacteria: a preliminary study. *J Nanomater* 2015; **2015**: 1–8.
24. Oda Y, Hayashi F, Wakita A, et al. Five-year longitudinal study of dental caries risk associated with *Streptococcus mutans* and *Streptococcus sobrinus* in individuals with intellectual disabilities. *J Oral Sci.* 2016;59:39–46.
25. De Soet JJ, Van Loveren C, Lammens AJ, et al. Differences in cariogenicity between fresh isolates of *Streptococcus sobrinus* and *Streptococcus mutans*. *Caries Res.* 1991;25:116–22.
26. Li Y, Caufield PW, Emanuelsson IR, et al. Differentiation of *Streptococcus mutans* and *Streptococcus sobrinus* via genotypic and phenotypic profiles from three different populations. *Oral Microbiol Immunol.* 2001;16:16–23.
27. Akrivopoulou C, Green IM, Donos N, et al. *Aggregatibacter actinomycetemcomitans* serotype prevalence and antibiotic resistance in a UK population with periodontitis. *J Glob Antimicrob Resist.* 2017;10:54–8.
28. Herbert BA, Novince CM, Kirkwood KL. *Aggregatibacter actinomycetemcomitans*, a potent immunoregulator of the periodontal host defense system and alveolar bone homeostasis. *Mol Oral Microbiol.* 2016;31:207–27.
29. Souto R, Silva-Boghossian CM, Colombo APV. Prevalence of *Pseudomonas aeruginosa* and *Acinetobacter* spp. in subgingival biofilm and saliva of subjects with chronic periodontal infection. *Braz J Microbiol.* 2014;45:495–501.
30. Grzech-Leśniak K, Matys J, Dominiak M. Comparison of the clinical and microbiological effects of antibiotic therapy in periodontal pockets following laser treatment: An in vivo study. *Adv Clin Exp Med.* 2018;27:1263–70.
31. Castro DT, Valente MLC, Aires CP, et al. Elemental ion release and cytotoxicity of antimicrobial acrylic resins incorporated with nanomaterial. *Gerodontology.* 2017;34:320–5.
32. Teixeira ABV, Castro DT, Schiavon MA, et al. Cytotoxicity and release ions of endodontic sealers incorporated with a silver and vanadium base nanomaterial. *Odontology* 2020; in press.
33. Anami LC, Pereira CA, Guerra E, et al. Morphology and bacterial colonization of tooth/ceramic restoration interface after different cement excess removal techniques. *J Dent.* 2012;40:742–9.
34. Ramakrishnaiah R, Alkheraif A, Divakar D, et al. The effect of hydrofluoric acid etching duration on the surface micromorphology, roughness, and wettability of dental ceramics. *Int J Mol Sci.* 2016;17:822.1–17.

35. Ayad MF, Fahmy NZ, Rosenstiel SF. Effect of surface treatment on roughness and bond strength of a heat-pressed ceramic. *J Prosthet Dent.* 2008;99:123–30.
36. Chang HH, Cheng CL, Huang PJ, et al.. Application of scanning electron microscopy and X-ray microanalysis: FE-SEM, ESEM-EDS, and EDS mapping for studying the characteristics of topographical microstructure and elemental mapping of human cardiac calcified deposition. *Anal Bioanal Chem.* 2014;406:359–66.
37. Uçar Y, Aysan Meriç I, Ekren O. Layered manufacturing of dental ceramics: fracture mechanics, microstructure, and elemental composition of lithography-sintered ceramic. *J Prosthodont.* 2019;28:310–8.
38. Rizkalla AS, Jones DW. Indentation fracture toughness and dynamic elastic moduli for commercial feldspathic dental porcelain materials. *Dent Mater.* 2014;20:198–206.

Figures

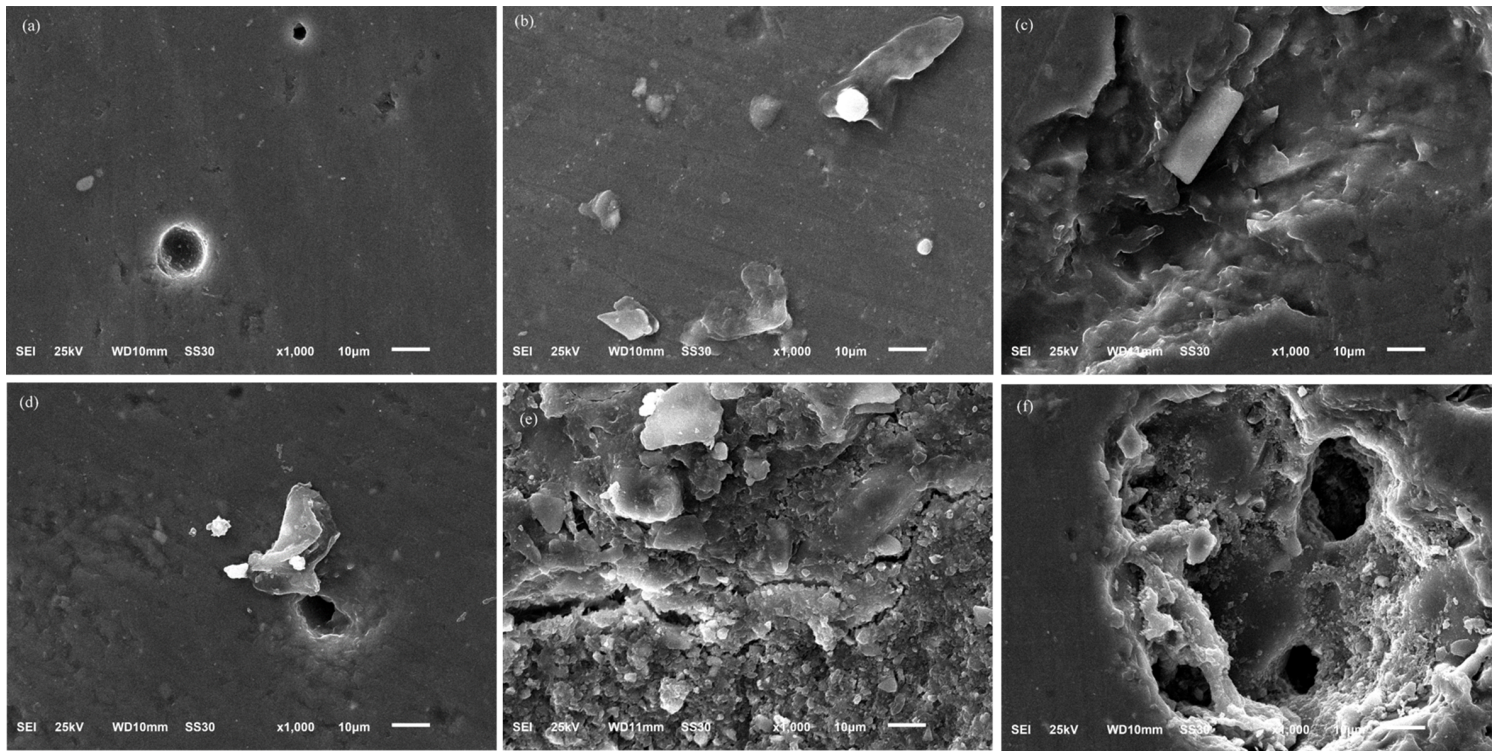


Figure 1

Photomicrographs of commercial dental porcelains incorporated with different concentrations of β -AgVO₃ (Magnification: 1000 x). (a) IPS Inline control. (b) IPS Inline incorporated with 2.5% of β -AgVO₃. (c) IPS Inline incorporated with 5% of β -AgVO₃. (d) Ex-3 Noritake control. (e) Ex-3 Noritake incorporated with 2.5% of β -AgVO₃. (f) Ex-3 Noritake incorporated with 5% of β -AgVO₃.

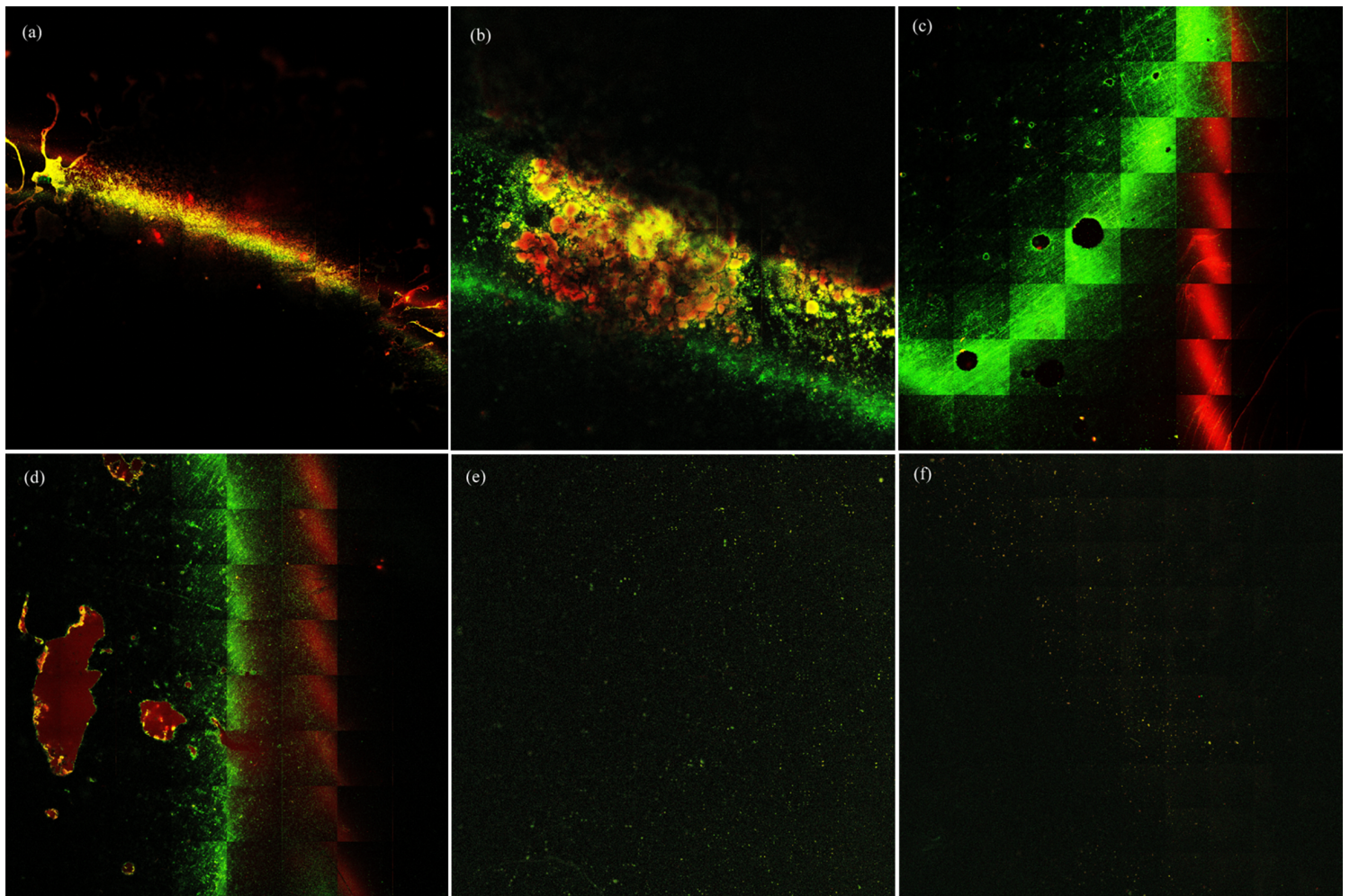


Figure 2

Photon images of biofilms of different microorganisms formed on the surface of dental porcelain IPS Inline incorporated with β -AgVO₃ acquired by multiphoton microscope. Green: viable cells (live), red: non-viable cells (dead). (a) *Streptococcus mutans* biofilm on the surface of control group. (b) *S. mutans* biofilm on the surface of 2.5% group. (c) *Streptococcus sobrinus* biofilm on the surface of control group. (d) *S. sobrinus* biofilm on the surface of 5% group. (e) *Aggregatibacter actinomycetemcomitans* biofilm on the surface of control group. (f) *A. actinomycetemcomitans* biofilm on the surface of 2.5% group.

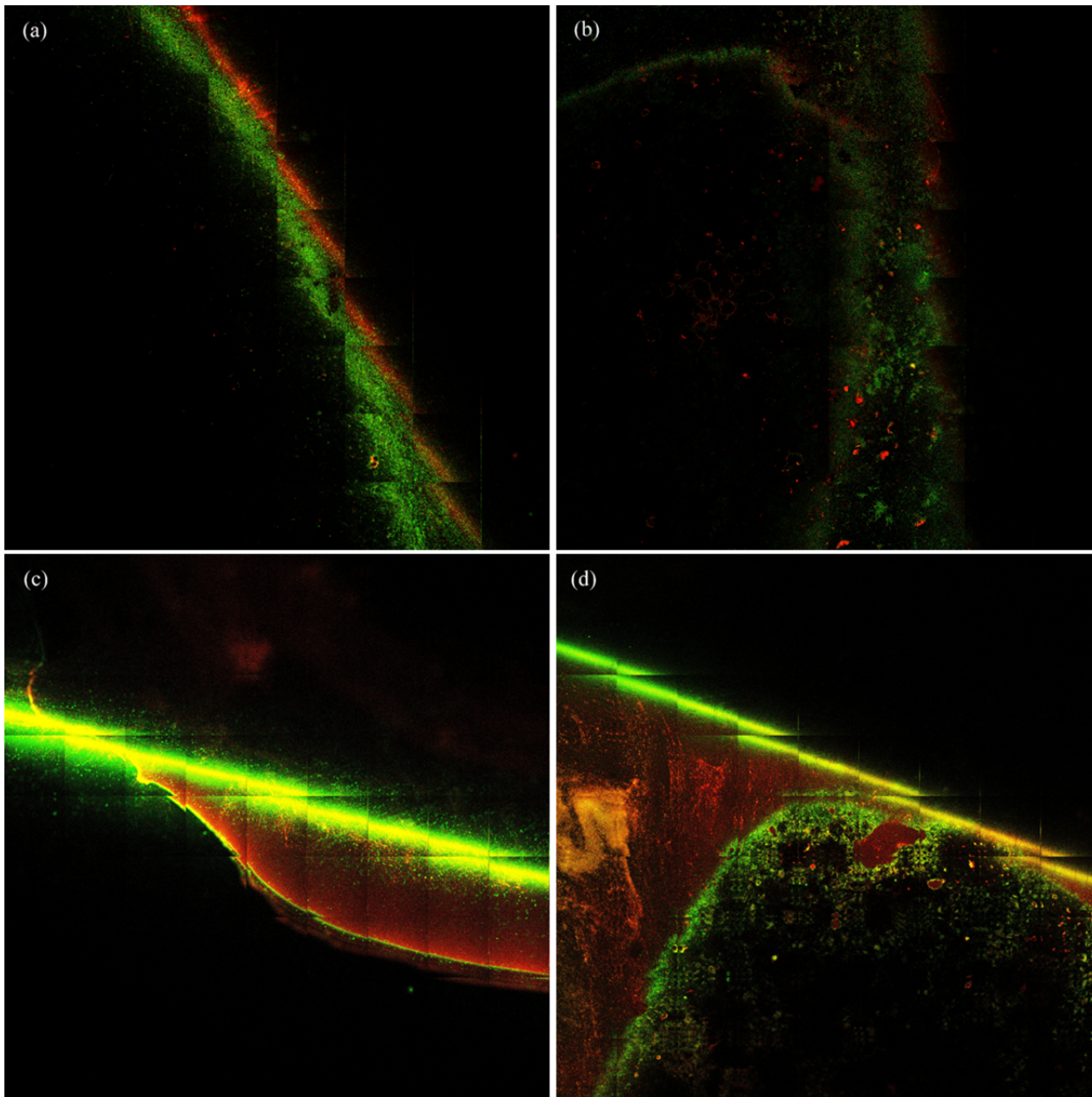


Figure 3

Photon images of biofilms of different microorganisms formed on the surface of dental porcelain Ex-3 Noritake incorporated with β -AgVO₃ acquired by multiphoton microscope. Green: viable cells (live), red: non-viable cells (dead). (a) *Streptococcus sobrinus* biofilm on the surface of control group. (b) *S. sobrinus* biofilm on the surface of 5% group. (c) *Pseudomonas aeruginosa* biofilm on the surface of control group. (d) *P. aeruginosa* biofilm on the surface of 5% group.